

G. Poelz

II. Institut für Experimentalphysik der Universität Hamburg*
2000 Hamburg 52 - Notkestrasse 85 - Germany

Summary

The Cerenkov counters in TASSO consist of 3 elements, one filled with aerogel and two with Freon 114 and CO₂. The 1700 liters of aerogel cover an area of 11.8m² with a thickness of 13.5 to 18 cm. Most cells are filled with an index of refraction between 1.023 and 1.026. In a running period of 2 months after installation $\langle N_e \rangle = 3.9 \pm 0.2$ photoelectrons were observed. The mean value over 17 months is $\langle N_e \rangle = 3.0 \pm 0.2$. The aerogel was manufactured at DESY with a rate of up to 90 l/week. The dimensions of the samples are 17 x 17 x 2.3 cm³. The refractive index of 986 pieces with n around 1.025 is distributed with $\sigma_n = 0.0013$. The transmission length for light with $\lambda_n = 438$ nm is $\Lambda = 2.64$ cm with $\sigma_\Lambda = 0.22$ cm. For 100 samples with n = 1.017, $\Lambda = 3.8$ cm with $\sigma_\Lambda = 0.6$ was found. In recent investigations the transmission length for aerogel with n = 1.025 could be improved to $\Lambda = 5.1$ cm.

The charged hadrons in the TASSO detector^{1,2} at PETRA are identified by time-of-flight counters and a Cerenkov system combined with the momentum information of the central detector. This Cerenkov system consists of 3 threshold counters filled with 1700 liters of aerogel, with Freon 114 and CO₂. All the aerogel was manufactured at DESY. This paper describes the method used for the production of aerogel, its performance and the properties of the Cerenkov detectors.

In aerogel small colloidal particles of silica with 4 nm in diameter are linked to branched strings. They form a porous structure with voids of about 20 to 200 nm in diameter. The index of refraction results from an average within a wavelength of light. It depends on the density ρ (g/cm³) of the aerogel by (Fig. 1)

$$n - 1 = (0.210 \pm 0.002) \cdot \rho$$

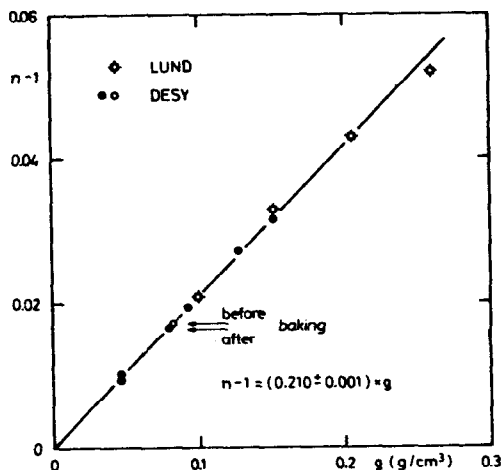
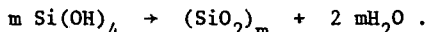
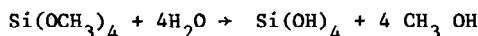


Fig. 1. Refractivity of silica aerogel produced at DESY and Lund as function of its density.

Preparation of aerogel

Aerogel for Cerenkov radiators is usually prepared out of tetramethoxisilan. It decomposes by hydrolyzation and then condensates to silica colloids



When grown to the right size ($m \sim 700$), the particle come into contact and are bound together (Fig. 2) forming a gel. It takes the same volume as the initial liquid mixture. If more or less methanol is added at the beginning, gels with different densities can be prepared and different indices of refraction are obtained.

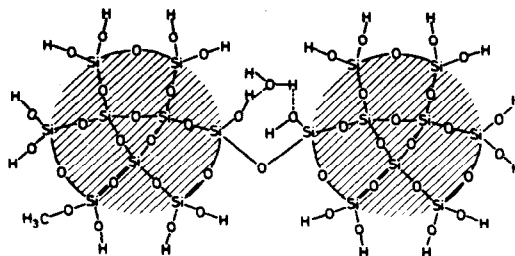


Fig. 2. Sketch of 2 colloidal particles bound by a siloxan link (Si-O-Si) and by a water bond.

The speed of gelation is in good approximation proportional to the concentration v_c (by volumes) of the added catalyst (NH₄OH)

$$1 / t_g = \alpha \cdot v_c$$

with the gelling time t_g . The coefficient α in turn depends linearly on the concentration v_s of the silan. From Fig. 3 one finds that below $v_s = 0.1$ no gelation takes place and refractive indices below $n = 1.01$ cannot directly be obtained with this mixing procedure.

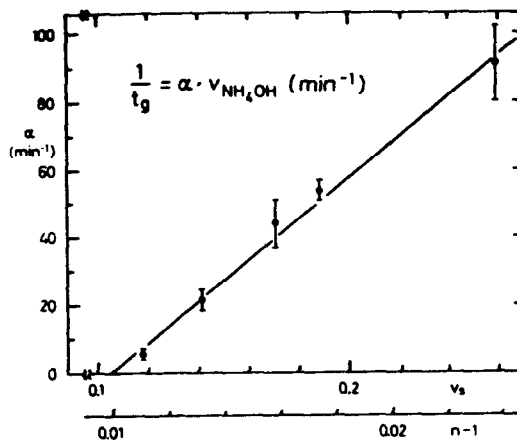


Fig. 3. Coefficient α of gelling speed $1/t_g$ as a function of the concentration v_s (by volumes) of the silan. The catalyst is a solution containing 25% ammonia. The concentration of this solution in the mixture is given by $v_{\text{NH}_4\text{OH}}$.

* Supported by the Deutsches Bundesministerium für Forschung und Technologie.

After gelation the pores of the gel are still completely filled with alcohol and water. To extract these liquids without harm to the delicate structure of the gel they have to be transferred into the gaseous phase (Fig. 4). The alcogel is heated in a pressure vessel slowly beyond the critical temperature (Fig. 5) and then the vapour is released at constant temperature. Now the gel can be cooled down and air penetrates the voids.

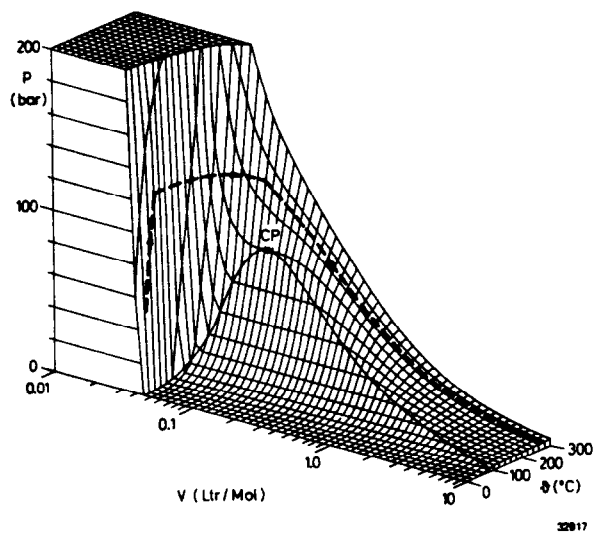


Fig. 4. Pressure-volume-temperature diagram for methanol calculated from the Redlich-Kwong equation modified to $p = RT/(V-b) - a/(\sqrt{T} V(V+c \cdot b))$. With $c = 15.97$ the parameters a and b are almost linear functions of the absolute temperature T . R is the gas constant. The extraction cycle in the autoclave follows the broken line.

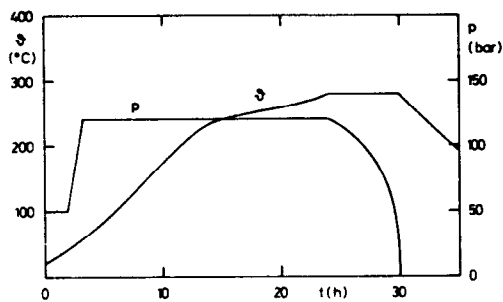


Fig. 5. Temperature and pressure inside the pressure vessel as a function of time. The rise in temperature and the decrease of the pressure take care of the changing density and viscosity of methanol.

Some residual methanol and water can be removed by baking the aerogel at 400°C in normal atmosphere for 3 hours. The optical properties of the gel is changed simultaneously. We find for samples with refractive indices around $n = 1.025$

$$n_i - n_f = 0.0065 - 0.15 (n_f - 1) = 0.003 \text{ for } n_f = 1.025$$

$$\mu_i - \mu_f = 0.27 - 0.45 \mu_f (\text{cm}^{-1}) = 0.1 \text{ cm}^{-1} \text{ for } \mu_f = 0.38 \text{ cm}^{-1}$$

The transmission coefficient μ was measured at a wavelength $\lambda = 436 \text{ nm}$ and i and f indicate the initial and final values.

Also the OCH_3 groups on the surface of the colloids are burned and OH groups remain. The initially hydrophobic aerogel is changed to a hydrophilic one.

The whole production cycle needs about 2 weeks for samples with $n = 1.025$. The freshly prepared gel should age at room temperature ($22 - 24^\circ\text{C}$) for about 10 days to strengthen the bonds between the colloidal particles. The bottle-neck in the production rate is the treatment in the pressure vessel. It takes 2 days.

At DESY we have 2 pressure vessels with a volume of 50 l each ($90 \text{ cm} \times 26 \text{ cm } \phi$). This allows a production rate of 100 to 140 samples per week with pieces of $17 \times 17 \times 2.3 \text{ cm}^3$ corresponding to 65 to 90 l/week.

The index of refraction and the transmission coefficient of each sample is measured. For 986 samples produced under similar conditions with n around 1.025 n is distributed with $\sigma_n = 0.0013$. The transmission length $\Lambda = 1/\mu$ was found to $\langle \Lambda \rangle = 2.64 \text{ cm}$ with $\sigma_\Lambda = 0.22 \text{ cm}$. The examination of 100 pieces with $n \sim 1.017$ yielded $\langle \Lambda \rangle = 3.8 \text{ cm}$ with $\sigma_\Lambda = 0.6 \text{ cm}$.

The refractivity measured at different points of the $17 \times 17 \text{ cm}^2$ surface of an aerogel sample is plotted in Fig. 6. The scatter of the values of about $\pm 5\%$ is mainly due to systematic uncertainties of the measurement because of the uneven surface of the sample.

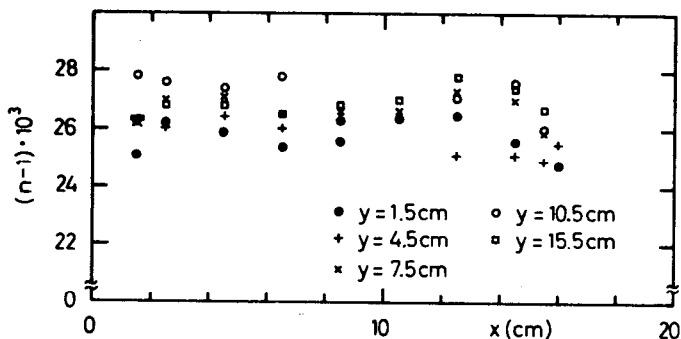


Fig. 6. Distribution of the refractivity in an aerogel sample across its surface of $17 \times 17 \text{ cm}^2$.

The scattering of light shows the expected λ^4 behaviour of Rayleigh scattering (Fig. 7). The absorption was measured by the decay time of the photon intensity within a diffuse reflecting box in the presence of aerogel. In the visible spectrum the absorption is smaller than the scattering. The corresponding lengths differ by at least one order of magnitude.

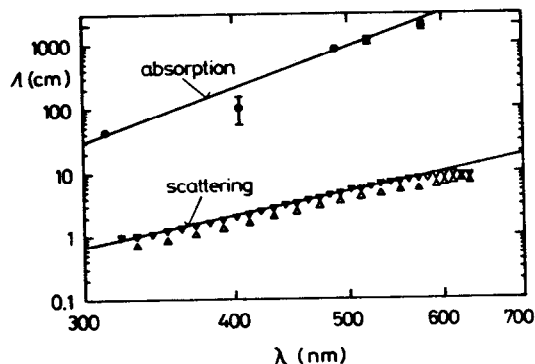


Fig. 7. Scattering length for unbaked (Δ) and baked (∇) aerogel and absorption length (\bullet) measured as a function of the wave length of light. The slope of the fitted lines is given by λ^4 and $\lambda^{6.7}$ respectively.

In recent experiments the transmission coefficient could be improved by a factor of 2 (Fig. 8). With a short gelling time t_g and chemicals cooled to 1°C a coefficient of $\mu = 0.2\text{ cm}^{-1}$ was obtained.

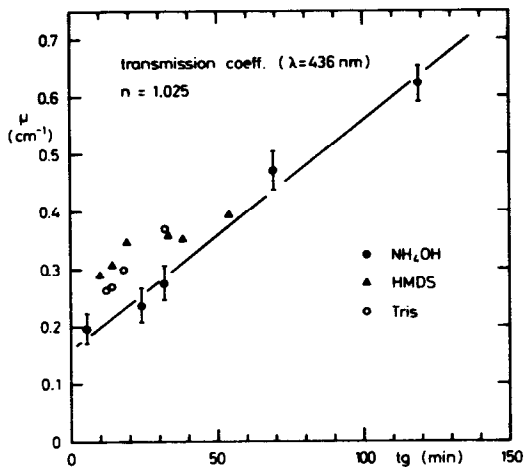


Fig. 8. Transmission coefficient μ as function of gelling time t_g at room temperature. As catalysts were used ammonia, hexamethyldisilazane and Tris(hydroxymethyl)-aminomethane. The left most point was obtained with a temperature of the liquids of 1°C ($t_g = 12\text{ min}$). Its position in the plot is scaled to room temperature.

All our samples were prepared in glass moulds and remained there also in the evaporation cycle. The moulds had to have rounded edges. With this shape the gel will not break when it detaches from the walls. We now succeeded to produce also aerogel with sharp edges without cracks. The gel is cast in a mould with removable walls (Fig. 9) and then transferred to a wider dish.

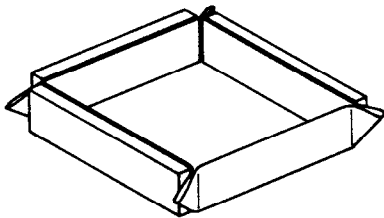


Fig. 9. Mould with removable walls to obtain aerogel slabs with sharp edges. A thin plastic foil separates the gel from the walls.

Aerogel-Cerenkov counters

The mean number of photoelectrons $\langle N_e \rangle$ detected by a phototube like RCA 8854 or XP 2041 in a Cerenkov counter can be estimated³ by

$$\langle N_e \rangle = n_0 \cdot \sin^2 \theta_c \cdot d_{\text{eff}} \cdot \eta_c$$

with $n_0 = 100\text{ cm}^{-1}$, the Cerenkov angle θ_c , the effective thickness of aerogel $d_{\text{eff}} = \Lambda(1 - \exp(-d/\Lambda))$, the real thickness d , and the light collection efficiency η_c (for Λ see below).

For the collection of the Cerenkov light two different systems are usually recommended:

With mirrors one may obtain a high collection efficiency, a particle with wrong direction is not detected and the signal is prompt.

But to put the mirrors in the right position space is needed and the highest collection efficiencies can only be reached with mirrors of complicated shapes. The collection efficiency tends to be inhomogeneous over the area of the aerogel.

Λ is determined by the transmission length of the aerogel $\Lambda \sim \Lambda_{\text{trans}} \sim 2-5\text{ cm}$ and η_c is limited by the reflectivity of the mirrors $\eta_c \leq 0.9$.

With diffuse reflecting walls one collects the direct and scattered light. The counter is easy to design and the collection efficiency is homogeneous. But to obtain a reasonable collection a high reflectivity is needed ($r \geq 0.95$). Photons with many reflections arrive within longer time intervals at the photomultiplier. The counter is sensitive to all particle directions.

The effective thickness of aerogel is here determined mainly by the absorption length Λ_a of the gel. $\Lambda \sim \Lambda_a \sim 11\text{ cm}$ and

$$\eta_c = t \cdot F / (1 - r(1 - F))$$

with the combined transmission of the light funnel and the photocathode $t = 0.4$ and F the fractional area of the photocathode $F = \text{area (PM)} / \text{area (total)}$.

In small counters a high yield is easily obtained. The counter in Fig. 10 with dimensions of $24 \times 20 \times (21.5 - 38)\text{ cm}^3$ was lined with millipore. With 18 cm of aerogel 12 photoelectrons were produced by relativistic electrons. The aerogel slabs had an index of refraction of 1.023 and were not baked.

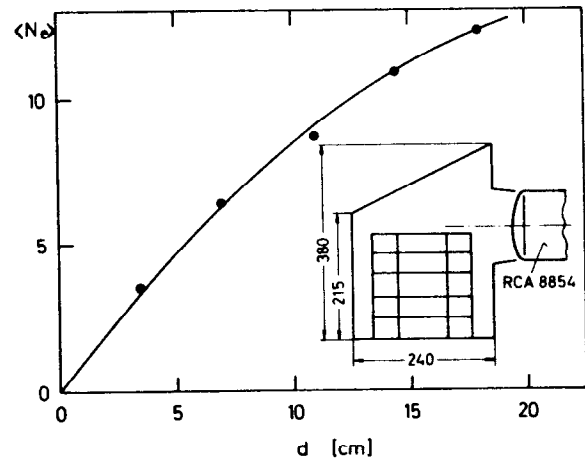


Fig. 10. Photoelectron yield of a small counter with diffuse reflecting walls and with different aerogel layers of thickness d . The counter was tested in a beam of relativistic electrons.

One cell of the aerogel Cerenkov detector used in TASSO is sketched in Fig. 11. The area of aerogel is about $35 \times 100\text{ cm}^2$. The long distance between the radiator and the photomultipliers was determined by the adjacent detector components. Monte Carlo computations for the different collection systems showed that the diffuse reflection scheme should be favoured. The total cell is lined with one layer of millipore. The aerogel slabs were cut with a diamond saw to the right shape and stacked into a drawer which is then inserted into the counter cell. The aerogel pieces

are held in place by cotton threads.

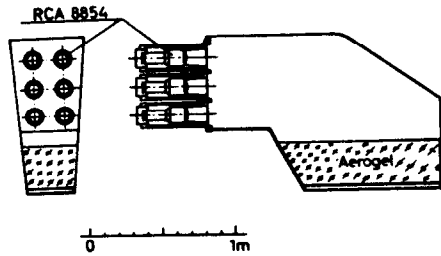


Fig. 11. Sketch of a detector cell used in TASSO.

A prototype was tested in pion beams at DESY and CERN. Fig. 12 shows the threshold curve for 18.5 cm of aerogel with $n = 1.024$. The signal below threshold is almost due to δ electrons. For the light produced in the millipore we found $2.4 \cdot 10^2$ photoelectrons.

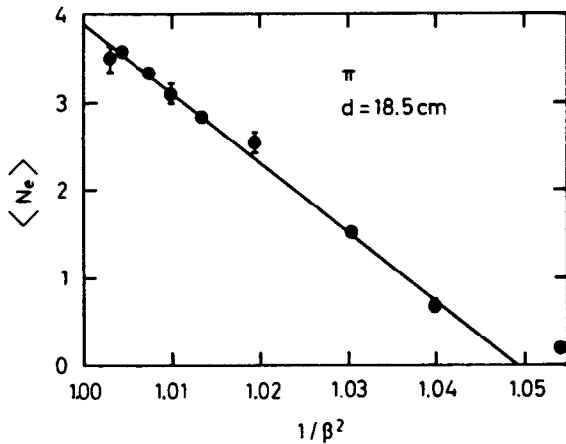


Fig. 12. Threshold curve for a TASSO cell like Fig. 11 tested in a pion beam.

The light yield was investigated in a beam of pions with a momentum of 3.4 GeV/c (Fig. 13). The data for different radiator thickness are fitted with an effective absorption length of $\Lambda_a = 9 \pm 1$ cm.

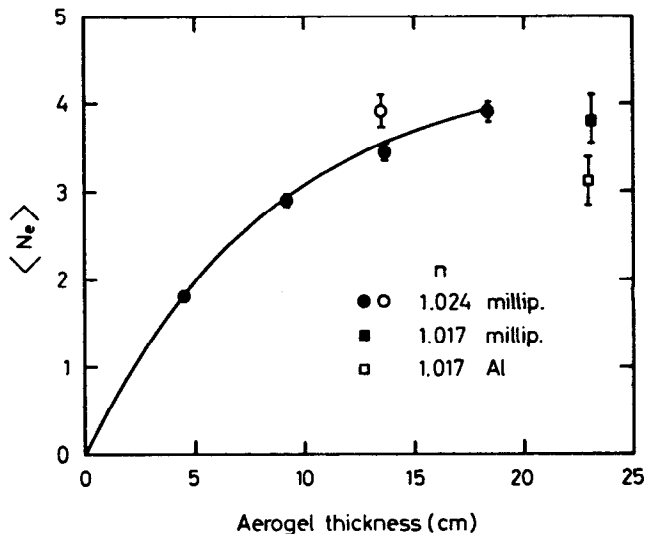


Fig. 13. Mean number of photoelectrons vs thickness of aerogel with $n=1.024$ (\bullet) measured with a TASSO cell. A pion beam of 3.4 GeV/c was used. The open point (\circ) gives the mean value from 16 cells with cosmic muons beyond 4 GeV/c. The squares are results with

$n = 1.017$ and cosmic muons ($p > 1.4$ GeV/c). The light was collected by millipore (\blacksquare) and aluminized mylar (\square).

In a measurement with aerogel of $n = 1.017$ in a layer of 23 cm thickness and cosmic muons ($p > 1.4$ GeV/c) we obtained a comparable yield of $\langle N \rangle = 3.9 \pm 0.3$ (Fig. 13). The lower number of Cerenkov photons is compensated by the higher transparency of the gel. With aluminized mylar at the walls and an appropriately bent foil opposite to the aerogel the yield decreased to 3.1 ± 0.1 photoelectrons.

The assembly of the 32 cells in the Cerenkov detector of TASSO is shown in Fig. 14. The Cerenkov counters are arranged in 2 horizontal arms and subtend a solid angle of 19% of 4π (see Table 1).

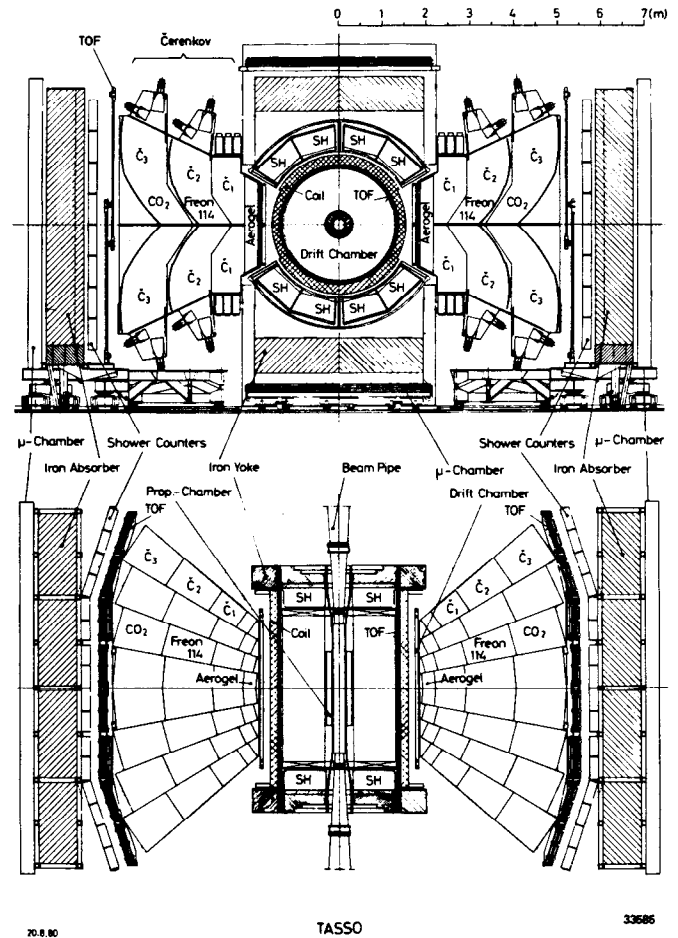


Fig. 14. End and top view of the TASSO detector.

The 16 cells below the mid plane can be tested by cosmic muons in parallel to the data taking runs. In the first 2 months after installation a yield of $\langle N_e \rangle = 3.9 \pm 0.2$ for particles with $p \geq 4$ GeV/c was observed.

Table 1 - The aerogel Cerenkov counters in TASSO

Solid angle	$19\% * 4\pi$
	$\theta = 90^\circ \pm 40^\circ$
	$\phi = \pm 26^\circ$
Substructure	32 cells
Area of aerogel	11.8 m^2
Volume of aerogel	1700 l
Aerogel thickness	$d = 13.5 \text{ cm}$ in 28 cells
	$d = 18.0 \text{ cm}$ in 4 cells
Index of refraction	$n = 1.023 \div 1.026$ in 24 cells
	$n = 1.020 \div 1.023$ in 8 cells.

The threshold curve for cosmic muons averaged over the whole run period (February 1979 to July 1981) is plotted in Fig. 15. The number of photoelectrons here reaches $\langle N_e \rangle = 3.0 \pm 0.2$. Fig. 16 shows the result of the evaluation of hadronic data. The fraction of charged particles seen by the aerogel counters relative to all candidates is plotted versus the particle momentum. The arrows indicate the threshold for π^- , K-mesons and protons. The solid line is computed assuming constant particle ratios. The effect of pions and kaons are clearly seen.

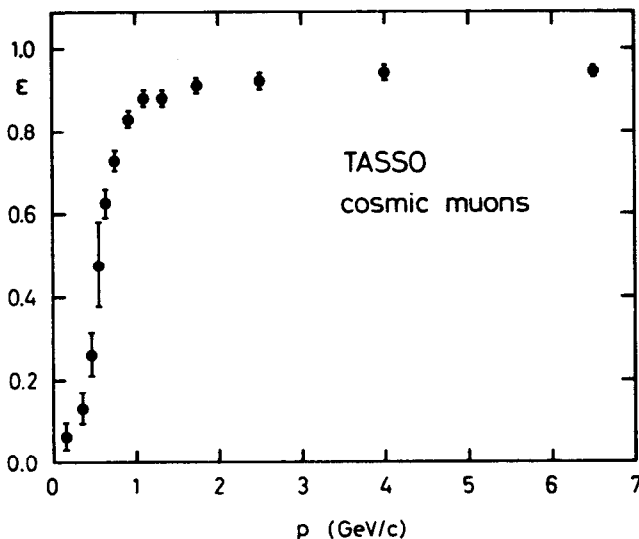


Fig. 15. Threshold curve for cosmic muons of all TASSO cells below the horizontal mid plane. The data are collected during 1.5 years parallel to the runs.

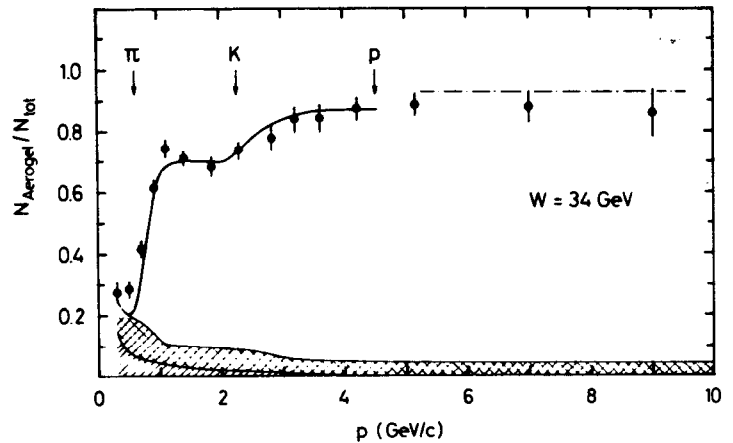


Fig. 16. Fraction of charged hadronic particles detected by the TASSO aerogel counters relative to all candidates. The arrows indicate the respective threshold. Dashed line: maximum limit caused by a software cut. A fast dropping electron background and a flat background from neighbouring showers is also shown.

References

- 1) TASSO Collaboration, R.Brandelik et al., "Properties of Hadron Final States in e^+e^- Annihilation at 13 GeV and 17 GeV Center of Mass Energies", Phys. Lett. 83B, 261 (1979)
- 2) H.Boerner, H.M.Fischer, H.Hartmann, B.Löhr, M.Wollstadt, D.G.Cassel, U.Kötz, H.Kowalski, B.H.Wiik, R.Fohrmann, and P.Schmüser, "The Large Cylindrical Drift Chamber of TASSO" Nucl.Instr. and Meth. 176, 151 (1980)
- 3) H.Burkhardt, P.Koehler, R.Riethmüller, B.H.Wiik, R.Fohrmann, J.Franzke, H.L.Krasemann, R.Maschuw, G.Poelz, J.Reichardt, J.Ringel, O.Römer, R.Rüsch, P.Schmüser, R.van Staa, J.Freeman, P.Lecomte, T.Meyer, Sau Lan Wu and G.Zobernig, "The TASSO Gas and Aerogel Cerenkov Counters" Nucl.Instr. and Meth. 184, 319 (1981)
- 4) G.Poelz and R.Riethmüller, "Preparation of Silica Aerogel for Cerenkov Counters" DESY preprint 81-055, to be published in Nucl.Instr. and Meth.
- 5) S.Henning and L.Svensson, "Production of Silica Aerogel", Physica Scripta 23, 697 (1981)
- 6) M.Cantin, M.Casse, L.Koch, R.Jouan, P.Mestreau, D.Roussel, F.Bonnin, J.Moutel and S.J.Teichner "Silica Aerogels used as Cerenkov Radiators" Nucl.Instr. and Meth. 118, 177 (1974)
- 7) Landolt - Börnstein New Series, ed. K.-H.Hellwege, IV, 3, p.18 (Springer-Verlag Berlin, Heidelberg, New York 1975)
- 8) TASSO Collaboration, to be published.